Agostic β-Si–H Interactions in Silylamido Complexes of Zirconocene

Leo J. Procopio,† Patrick J. Carroll, and Donald H. Berry*

Contribution from the Department of Chemistry and Laboratory for Research on the Structure of Matter, University of Pennsylvania, Philadelphia, Pennsylvania 19104-6323

Received September 3, 1993®

Abstract: A series of silylamido complexes of zirconium, $Cp_2Zr(X)(N^tBuSiMe_2H)$ (X = H, I, Br, Cl, F; **1–5**), have been prepared. These complexes exhibit agostic β-Si–H interactions with the metal center and have been characterized by spectroscopic and structural methods. Spectroscopic evidence for the interaction of the Si–H σ-bond with zirconium include (1) abnormally large upfield chemical shifts for the silicon hydride and silicon nuclei in the ^1H and ^{29}Si NMR spectra, (2) unusually small values of the silicon–hydrogen coupling constants ($^1J_{SiH}$), and (3) low-energy Si–H stretching frequencies in the infrared spectra. All of the spectroscopic data also establish a clear trend for the strength of the nonclassical Zr–H–Si interaction in $Cp_2Zr(X)(N^tBuSiMe_2H)$: X = H > I > Br > Cl > F. This ordering directly reflects the relative electrophilicity of the zirconium center. The molecular structures of the hydride and chloride derivatives **1** and **4** as determined by single-crystal X-ray diffraction studies are also consistent with coordination of the Si–H bond to the metal center. In particular, short Zr–Si distances and acute Zr–N–Si angles point to a severe bending of the silyl group toward zirconium, and the location of the amido group near the center of the metallocene equatorial wedge is consistent with a Cp_2ML_3 coordination environment, not the Cp_2ML_2 geometry implied by the formula $Cp_2Zr(NR_2)(X)$.

Introduction

The observation and isolation of metal complexes of "nonclassical" ligands such as dihydrogen[1] and saturated hydrocarbons[1e,2,3] have forced organometallic chemists to expand their inventory of viable ligands well beyond traditional donors. The study of nonclassical ligands has also yielded insight into the important processes of H–H and C–H bond activation, and in a practical sense such σ-bond complexes have proven important in determining the outcome of C–C bond-forming reactions in Ziegler–Natta olefin polymerization[4] and as an indicator of the activity of cobalt ethylene polymerization catalysts.[5]

Interestingly, substantial spectroscopic and structural evidence for three-center Si–H–M complexes[6–8] had been amassed well before the advent of the term "agostic" to describe C–H bond complexes,[2a] and prior to the discovery of nonclassical hydrogen complexes,[1] although the obvious relevance to H–H and C–H complexes remained overlooked for many years. The most extensively studied system involving η^2-coordination of Si–H bonds has been the series of manganese complexes $(\eta^5\text{-}C_5R_5)Mn(L)_2(\eta^2\text{-}HSiR_3)$.[7] Indeed, σ-bonds involving silicon in general appear to be particularly good electron donors toward transition metals, and nonclassical Si–C and Si–Cl complexes are also known.[9]

In general, the bonding in σ-bond complexes is best described in terms of two principal interactions: a σ-type interaction between

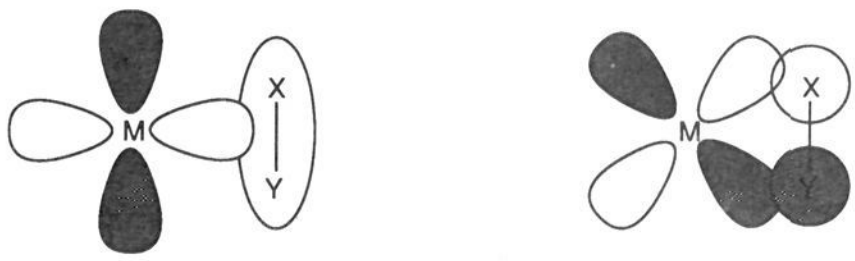

σ π

the σ-orbital of the ligand (XY) and a vacant metal orbital of appropriate symmetry and a π-type interaction between a filled

† Present address: Research Laboratories, Rohm and Haas Co., Spring House, PA 19477.

® Abstract published in *Advance ACS Abstracts,* December 15, 1993.

(1) For example, see: (a) Kubas, G. J.; Ryan, R. R.; Swanson, B. I.; Vergamini, P. J.; Wasserman, H. J. *J. Am. Chem. Soc.* **1984**, *106*, 451. (b) Kubas, G. J.; Unkefer, C. J.; Swanson, B. I.; Fukushima, E. *J. Am. Chem. Soc.* **1986**, *108*, 7000. (c) Gadd, G. E.; Upmacis, R. K.; Poliakoff, M.; Turner, J. J. *J. Am. Chem. Soc.* **1986**, *108*, 2547. (d) Crabtree, R. H.; Lavin, M.; Bonnevoit, L. *J. Am. Chem. Soc.* **1986**, *108*, 4032. For recent reviews, see: (e) Crabtree, R. H.; Hamilton, D. G. *Adv. Organomet. Chem.* **1988**, *28*, 299. (f) Heinekey, D. M.; Oldham, W. J. *Chem. Rev.* **1993**, *93*, 913.

(2) (a) Brookhart, M.; Green, M. L. H. *J. Organomet. Chem.* **1983**, *250*, 395. (b) Brookhart, M.; Green, M. L. H.; Wong, L.-L. *Prog. Inorg. Chem.* **1988**, *36*, 1.

(3) For example, see: (a) Fellmann, J. D.; Schrock, R. R.; Traficante, D. D. *Organometallics* **1982**, *1*, 481. (b) Benn, R.; Holle, S.; Jolly, P. W.; Mynott, R.; Romão, C. C. *Angew. Chem., Int. Ed. Engl.* **1986**, *25*, 555. (c) Hyla-Kryspin, I.; Gleiter, R.; Krüger, C.; Zwettler, R.; Erker, G. *Organometallics* **1990**, *9*, 517. (d) Bullock, R. M.; Lemke, F. R.; Szalda, D. J. *J. Am. Chem. Soc.* **1990**, *112*, 3244.

(4) (a) Burger, B. J.; Thompson, M. E.; Cotter, W. D.; Bercaw, J. E. *J. Am. Chem. Soc.* **1990**, *112*, 1566. (b) Piers, W. E.; Bercaw, J. E. *J. Am. Chem. Soc.* **1990**, *112*, 9406. (c) Prosenc, M. H.; Janiak, C.; Brintzinger, H. H. *Organometallics* **1992**, *11*, 4036. (d) Krauledat, H.; Brintzinger, H. H. *Angew. Chem., Int. Ed. Engl.* **1990**, *29*, 1412. (e) Janiak, C. *J. Organomet. Chem.* **1993**, *452*, 63.

(5) (a) Brookhart, M.; Schmidt, G. F. *J. Am. Chem. Soc.* **1985**, *107*, 1443. (b) Brookhart, M.; Volpe, A. F.; Lincoln, D. M. *J. Am. Chem. Soc.* **1990**, *112*, 5634.

(6) For a recent review, see: Schubert, U. *Adv. Organomet. Chem.* **1990**, *30*, 151.

(7) For example, see: (a) Jetz, W.; Graham, W. A. G. *Inorg. Chem.* **1971**, *10*, 4. (b) Colomer, E.; Corriu, R. J. P.; Marzin, C.; Vioux, A. *Inorg. Chem.* **1982**, *21*, 368. (c) Schubert, U.; Ackermann, K.; Wörle, B. *J. Am. Chem. Soc.* **1982**, *104*, 7378. (d) Carrè, F. Colomer, E.; Corriu, R. J. P.; Vioux, A. *Organometallics* **1984**, *3*, 1272. (e) Kraft, G.; Kalbas, C.; Schubert, U. *J. Organomet Chem.* **1985**, *289*, 247. (f) Schubert, U.; Scholz, G.; Müller, J.; Ackermann, K.; Wörle, B.; Stansfield, R. F. D. *J. Organomet. Chem.* **1986**, *306*, 303.

(8) (a) Bennett, M. J.; Simpson, K. A. *J. Am. Chem. Soc.* **1971**, *93*, 7156. (b) Auburn, M.; Ciriano, M.; Howard, J. A. K.; Murray, M.; Pugh, N. J.; Spencer, J. L.; Stone, F. G. A.; Woodward, P. *J. Chem. Soc., Dalton Trans.* **1980**, 659. (c) Aitken, C. T.; Harrod, J. F.; Samuel, E. *J. Am. Chem. Soc.* **1986**, *108*, 4059. (d) Suzuki, H.; Takao, T.; Tanaka, M.; Moro-oka, Y. *J. Chem. Soc., Chem. Commun.* **1992**, 476.

(9) For example, see: (a) Tilley, T. D.; Andersen, R. A.; Zalkin, A. *Inorg. Chem.* **1984**, *23*, 2271. (b) Tilley, T. D.; Andersen, R. A.; Zalkin, A. *J. Am. Chem. Soc.* **1982**, *104*, 3725. (c) Boncella, J. M.; Andersen, R. A. *Organometallics* **1985**, *4*, 205. (d) Evans, W. J.; Drummond, D. K.; Zhang, H.; Atwood, J. L. *Inorg. Chem.* **1988**, *27*, 575. (e) Jeske, G.; Schock, L. E.; Sweptson, P. N.; Schumann, H.; Marks, T. J. *J. Am. Chem. Soc.* **1985**, *107*, 8103. (f) Heeres, H. J.; Meetsma, A.; Teuben, J. H.; Rogers, R. D. *Organometallics* **1989**, *8*, 2637. (g) Van der Heijden, H.; Schaverien, C. J.; Orpen, A. G. *Organometallics* **1989**, *8*, 255. (h) Horton, A. D.; Orpen, A. G. *Organometallics* **1992**, *11*, 1193.

0002-7863/94/1516-0177$04.50/0 © 1994 American Chemical Society

metal d-orbital and the σ^*-orbital of XY. Both interactions lead to a reduction in the X–Y bond order and, in the extreme limit, result in complete bond cleavage and formation of the classical oxidative-addition product, M(X)(Y). Thus, compounds which contain coordinated σ-bonds in their ground states can be viewed as "frozen" intermediates along the oxidative-addition pathway.

The majority of η^2-silane complexes characterized to date are mononuclear species containing relatively simple silanes (**A**), although several examples of dinuclear metal complexes with bridging M–H–Si interactions (**B**) have been described.[8]

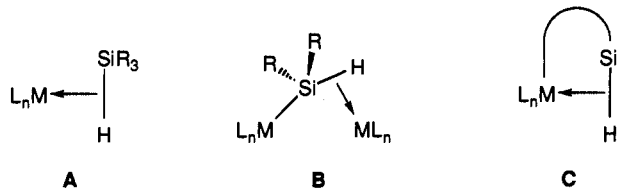

We now report the preparation and spectroscopic and structural characterization of a series of zirconocene amides, $Cp_2Zr(X)(N^tBuSiMe_2H)$ ($Cp \equiv \eta^5$-C_5H_5; X = H, I, Br, Cl, F), in which the pendant silyl group is coordinated to the metal via an η^2-Si–H interaction. In addition, trends in a wide range of spectroscopic parameters clearly establish a correlation between the strength of the nonclassical interaction and the effective electron density at the metal center. The zirconocene complexes described in this contribution are unusual examples of mononuclear η^2-silane complexes containing chelating Si–H bonds (**C**). The only other example of this bonding mode was recently reported for the zirconium amide $\{Zr(Cl)(\mu\text{-}Cl)[N(SiMe_2H)_2]_2\}_2$.[10]

Results and Discussion

Synthesis of the Zirconocene Amides $Cp_2Zr(X)(N^tBuSiMe_2H)$. We have previously described the reaction of $[Cp_2ZrHCl]_n$ and $LiN^tBuSiMe_2H{\cdot}THF$ in benzene, which produces the silylamido complex $Cp_2Zr(H)(N^tBuSiMe_2H)$ (**1**) in good yields (86%, eq 1).[11] Compound **1** has been fully characterized by multinuclear

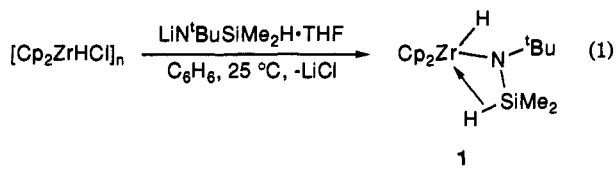

NMR, elemental analysis, MS, and solution molecular weight measurements. Interestingly, the last indicate a monomeric, rather than a dimeric, structure for **1**, which is unprecedented for a formally 16e$^-$ zirconocene hydride containing the relatively unhindered η^5-C_5H_5 rings. The monomeric nature of **1** has been conclusively established by a single-crystal X-ray diffraction study (vide infra).

Treatment of hydride **1** with ca. 1 equiv of methyl iodide in toluene solution rapidly generates the iodide derivative $Cp_2Zr(I)(N^tBuSiMe_2H)$ (**2**) and methane.[11] The reaction is complete after <2 h at room temperature. Similar methods have been utilized in the synthesis of the other halide derivatives (Scheme 1). For example, **1** undergoes bromination upon reaction with ca. 5 equiv of dibromomethane in benzene solution, cleanly producing $Cp_2Zr(Br)(N^tBuSiMe_2H)$ (**3**) and presumably CH_3Br. The reaction is complete within 2 days at room temperature. Chlorination occurs slowly in the reaction of **1** with methyl chloride (ca. 10 equiv), yielding the chloride $Cp_2Zr(Cl)(N^tBuSiMe_2H)$

(10) Herrmann, W. A.; Huber, N. W.; Behm, J. *Chem. Ber.* **1992**, *125*, 1405.

(11) (a) Procopio, L. J.; Carroll, P. J.; Berry, D. H. *J. Am. Chem. Soc.* **1991**, *113*, 1870. (b) Procopio, L. J. Ph.D. Thesis, University of Pennsylvania, 1991.

Scheme 1

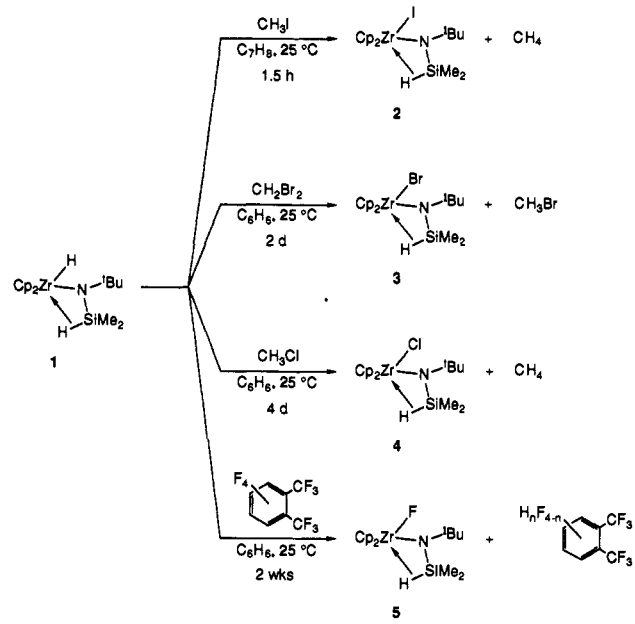

(**4**) and presumably methane. The reaction proceeds rather sluggishly, requiring 4 days for completion at 25 °C.

Although formation of halide derivatives **2**–**4** was rather straightforward and in each case led to high isolated yields, the synthesis of the fluoride proved somewhat more difficult. Fluorination of **1** with perfluorobenzene led to a complex mixture of products, containing <50% of the desired $Cp_2Zr(F)(N^tBuSiMe_2H)$ (**5**), as well as unreacted starting material. Attempts to extract pure **5** from this mixture were unsuccessful. However, use of a more sterically hindered fluorinating agent, perfluoro-*o*-xylene, led to a less complicated mixture from which **5** was isolated as a white solid in 51% yield after recrystallization.

Compounds **1**–**5** display a variety of spectroscopic properties which allow their characterization as complexes containing agostic Si–H interactions. In addition, X-ray structural determinations for the parent hydride, $Cp_2Zr(H)(N^tBuSiMe_2H)$ (**1**), and the chloride, $Cp_2Zr(Cl)(N^tBuSiMe_2H)$ (**4**), confirm the presence of the nonclassical bonding mode.

Spectroscopic Characterization of $Cp_2Zr(X)(N^tBuSiMe_2H)$. The first indication of an unusual bonding mode for the Si–H group in **1**–**5** is provided by ^{1}H NMR spectroscopy. The ^{1}H NMR spectrum of **1** exhibits resonances for the Cp (δ 5.69), ^{t}Bu (δ 1.23), and $SiMe_2$ (δ 0.04, d, $^3J_{HH}$ = 2.8 Hz) groups, but a peak for the Si–H group was not observed in the region normally associated with hydrogens bound to silicon (~3.5–5 ppm). Selective decoupling experiments have established that the Si–H resonance occurs at δ 1.21 and is partially obscured by the ^{t}Bu resonance. The chemical shift of the Si–H hydrogen is thus >2 ppm upfield of the resonances of normal silicon hydrides, indicating a significant perturbation of the Si–H environment. Significantly, the Zr–H resonance (δ 5.53) is observed as a *doublet* (J = 3.1 Hz), due to coupling with the silicon hydride. This would be an extremely large coupling constant for a simple four-bond interaction (i.e., H–Zr–N–Si–H), but is consistent with the presence of an agostic Si–H interaction with the zirconium, such that coupling of the ZrH and SiH protons occurs via a two-bond pathway (i.e., H–Zr–HSi).

The ^{19}F NMR spectrum of fluoride **5** displays a doublet (J_{FH} = 8.1 Hz) at δ 51.72.[12] Confirmation that fluorine is coupled to the silicon hydride comes from the ^{1}H NMR spectrum of **5** in which the $SiMe_2$ resonance is selectively decoupled, yielding a doublet (J_{FH} = 8.1 Hz) for the SiH resonance. Although coupling

(12) For comparison, $Cp_2Zr(F)_2$ displays a resonance at δ 30.7 in the ^{19}F NMR spectrum (benzene-d_6).

Table 1. Spectroscopic Data for $Cp_2Zr(X)(N^tBuSiMe_2H)$

compound	^1H NMR[a] δ_{SiH}	^{29}Si NMR[a] δ_{Si}	^{29}Si NMR[a] $^1J_{SiH}$	IR[b] ν_{SiH}
$Cp_2Zr(H)(N^tBuSiMe_2H)$ (**1**)	1.21	−73.4	113.2	1912
$Cp_2Zr(I)(N^tBuSiMe_2H)$ (**2**)	1.69	−62.0	118.7	1960
$Cp_2Zr(Br)(N^tBuSiMe_2H)$ (**3**)	2.24	−56.1	123.2	1975
$Cp_2Zr(Cl)(N^tBuSiMe_2H)$ (**4**)	2.58	−52.3	126.5	1981
$Cp_2Zr(F)(N^tBuSiMe_2H)$ (**5**)	2.84	−42.0	135.4	1998
$HN^tBuSiMe_2H$	4.83	−18.3	192.6	2107

[a] NMR spectra recorded in benzene-d_6 at 25 °C. Chemical shifts in ppm and $^1J_{SiH}$ in Hz. [b] IR spectra recorded in benzene solution at 25 °C. Values of ν_{SiH} in cm^{-1}.

of the silicon hydride and fluorine nuclei establishes that there is an interaction between the two atoms, it is not clear whether the magnitude of J_{FH} is more consistent with a four-bond (i.e., F–Zr–N–Si–H) or a two-bond (i.e., F–Zr–HSi) coupling, as no relevant data exist for comparison. Several known examples of zirconocene fluoride complexes do not exhibit ^{19}F–^1H coupling (e.g., $Cp^*_2Zr(H)(F)$ ($^2J_{FH} \approx 0$),[13] $Cp_2Zr(CH_3)(F)$ ($^3J_{FH} \approx 0$),[14] and $Cp^*_2Zr(CH_2CMe_3)(F)$ ($^3J_{FH} \approx 0$)[15]). In analogy to the coupling of the zirconium and silicon hydrides found for **1** and on the basis of additional spectroscopic evidence described below, it is proposed that the fluorine–hydrogen coupling in **5** occurs via the metal by a two-bond pathway (i.e., F–Zr–HSi).

The ^1H NMR spectra of halides **2–5** all display resonances for the Cp, ^{t}Bu, and $SiMe_2$ groups in the normal regions of the spectrum. However, as observed for **1**, the chemical shift of the SiH hydrogen (δ_{SiH}) in each of the derivatives is significantly upfield of the resonances of normal silicon hydrides (see Table 1) and is indicative of interaction with the metal. The SiH resonances in **1–5** follow a smooth progression, in which fluoride **5** has the furthest downfield resonance (δ 2.84). For comparison, the parent silylamine, $HN^tBuSiMe_2H$, displays a septet for the SiH proton at δ 4.87 in the ^1H NMR spectrum. The ^1H NMR data for compounds **1–5** suggest the following order for the decreasing degree of agostic bonding between the Si–H σ-bond and the zirconium center of $Cp_2Zr(X)(N^tBuSiMe_2H)$: X = H > I > Br > Cl > F. This order assumes that an upfield shift in δ_{SiH} reflects a stronger interaction with the metal.

The same trend is also apparent in the ^{29}Si NMR data for compounds **1–5** (Table 1). The ^{29}Si chemical shift of **1** (δ −73.4) is unexpectedly far upfield, being greater than 55 ppm further upfield than that found for the parent silylamine, $HN^tBuSiMe_2H$ (δ −18.3). This chemical shift is very similar to that observed for the η^2-silanimine complex $Cp_2Zr(\eta^2\text{-}SiMe_2{=}N^tBu)(CO)$ (δ −69.9),[11,16] in which there is a direct Zr–Si bond, suggesting a close contact between the Zr and Si atoms in **1**. The bonding of silicon to a transition metal is well-known to cause dramatic changes in the ^{29}Si chemical shift,[17] although it should be noted that resonances for Si atoms in small rings are also generally found upfield.[18] For instance, silaziridines (*c*-Si–C–N) exhibit ^{29}Si shifts approximately 90 ppm upfield of $SiMe_4$.[19] Thus the unusual ^{29}Si shift for **1** could be due to either close Zr–Si contact or distortion of the geometry at silicon, as in a small ring.

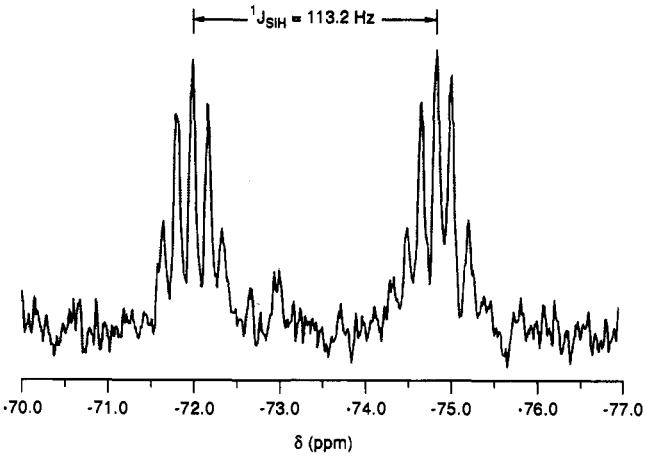

Figure 1. ^{29}Si (^1H coupled) NMR spectrum of $Cp_2Zr(H)(N^tBuSiMe_2H)$ (**1**).

As in the case of **1**, the ^{29}Si resonances (δ_{Si}) for the halide derivatives **2–5** appear far upfield from resonances of the parent silylamine $HN^tBuSiMe_2H$ (Table 1). The furthest downfield shift is that of fluoride **5** (δ −42.0), which is still more than 20 ppm upfield from that of $HN^tBuSiMe_2H$. A clear progression of δ_{Si} is observed for the hydride and halide derivatives **1–5**, with the fluoride derivative **5** exhibiting the least unusual shift and **1** exhibiting the most perturbed.

Perhaps the most striking feature of the ^{29}Si NMR spectra of **1–5** is the magnitude of the ^1H–^{29}Si coupling constants. The ^1H-coupled ^{29}Si resonances appear as doublets of septets, as illustrated by the spectrum of **1** (Figure 1). Although the coupling between the Si atom and methyl protons is normal for two-bond couplings ($^2J_{SiH} \approx 6$ Hz), the one-bond coupling is unusually small ($^1J_{SiH}$ = 113.2 Hz). Compounds **2–5** also exhibit small values of $^1J_{SiH}$ (118.7–135.4 Hz; see Table 1). Silicon hydrides generally display $^1J_{SiH}$ in the range 160–200 Hz.[20] Consider, for example, the $^1J_{SiH}$ value observed for the parent silylamine $HN^tBuSiMe_2H$ (192.6 Hz). The reduction of the one-bond coupling constant in the zirconium silylamides suggests a significant lengthening or rehybridization of the Si–H bond. Low values of $^1J_{SiH}$ have been specifically identified in a number of η^2-silane complexes,[6] most notably the manganese compounds $(\eta^5\text{-}C_5R_5)\text{-}Mn(L)_2(\eta^2\text{-}HSiR_3)$.[7] A similar reduction in $^1J_{CH}$ has been observed for metal complexes containing agostic C–H bonds,[2b] and the ^1H–^2H coupling in η^2-H_2 complexes (as measured in the η^2-HD analogs) is also substantially reduced from that in free dihydrogen.[1,21]

Hydride derivative **1** displays the smallest value of $^1J_{SiH}$ (113.2 Hz) for the series of zirconocene amides and thus again appears to exhibit the greatest degree of interaction between the metal and the silicon hydride. The highest value of $^1J_{SiH}$ (135.4 Hz) is observed for fluoride derivative **5**, although this value still falls well short of the normal range. The other derivatives display a smooth progression of intermediate values.

Compound **5** also exhibits coupling between the ^{29}Si and ^{19}F nuclei. The $^{29}Si\{^1H\}$ NMR spectrum of **5** clearly displays a doublet, yielding a ^{29}Si–^{19}F coupling constant (J_{SiF}) of 5.1 Hz. There are no values for obvious model compounds with which this value can be compared, and thus interpretation of the magnitude is difficult. The coupling constant is outside the range

(13) The ^{19}F NMR spectrum of $Cp^*_2Zr(H)(F)$ in benzene-d_6 displays a singlet at δ 71.11, and the ^1H NMR spectrum exhibits singlets at δ 6.61 (ZrH) and 1.91 (Cp*). The preparation of $Cp^*_2Zr(H)(F)$ is described in the literature: Barger, P. T.; Bercaw, J. E. *Organometallics* **1984**, *3*, 278.

(14) Jordan, R. F. *J. Organomet. Chem.* **1985**, *294*, 321.

(15) Wochner, F.; Brintzinger, H. H. *J. Organomet. Chem.* **1986**, *309*, 65.

(16) Procopio, L. J.; Carroll, P. J.; Berry, D. H. Manuscript in preparation.

(17) For example, see: (a) Pannell, K. H.; Bassindale, A. R. *J. Organomet. Chem.* **1982**, *229*, 1. (b) Pannell, K. H.; Rozell, J. M.; Tsai, W.-M. *Organometallics* **1987**, *6*, 2085.

(18) (a) Seyfert, D.; Annarelli, D. C.; Vick, S. C. *J. Am. Chem. Soc.* **1976**, *98*, 6382. (b) Seyfert, D.; Annarelli, D. C.; Vick, S. C.; Duncan, D. P. *J. Organomet. Chem.* **1980**, *201*, 179. (c) Ishikawa, M.; Sugisawa, H.; Kumada, M.; Higuchi, T.; Matsui, K.; Hirotsu, K.; Iyoda, J. *Organometallics* **1983**, *2*, 174. (d) Seyfert, D.; Annarelli, D. C.; Vick, S. C. *J. Organomet. Chem.* **1984**, *272*, 123. (e) Brook, A. G.; Wessely, H.-J. *Organometallics* **1985**, *4*, 1487. (f) Brook, A. G.; Saxena, A. K.; Sawyer, J. F. *Organometallics* **1989**, *8*, 850.

(19) Brook, A. G.; Kong, Y. K.; Saxena, A. K.; Sawyer, J. F. *Organometallics* **1988**, *7*, 2245.

(20) Williams, E. A.; Cargioli, J. D. In *Annual Reports on NMR Spectroscopy*; Webb, G. A., Ed.; Academic Press: New York, 1979; Vol. 9, p 221.

(21) Conroy-Lewis, F. M.; Simpson, S. J. *J. Chem. Soc., Chem. Commun.* **1986**, 506.

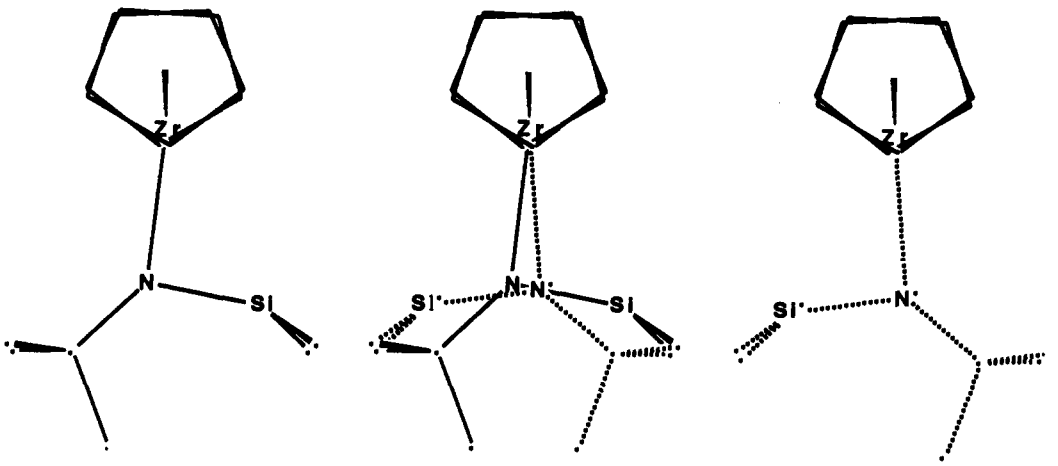

Figure 2. Depiction of disorder in the crystal structure of $Cp_2Zr(H)(N^tBuSiMe_2H)$ (**1**), viewed down through the two Cp rings. The two independent conformers are to the left and right, and their superposition is in the middle. Note that the Cp_2Zr fragment is invariant in both configurations and that the silicon methyl carbons and two of the *t*-Bu methyl carbons are shared in the superposition. The Zr and the nitrogen and silicon sites are coplanar.

of normal $^2J_{SiF}$ values (20–50 Hz) found for a number of fluorinated organosilanes.[22]

Coordination of a σ-bond (X–Y) to a transition metal often results in a significant weakening of the bond. This reduction in bond order has been demonstrated, especially for η^2-dihydrogen complexes,[1] by a decrease in the stretching frequency of the X–Y bond in the infrared spectrum. Similarly, evidence for η^2-Si–H coordination in the silylamido complexes is found in the infrared spectra of **1–5**. For example, the infrared spectrum of hydride **1** exhibits two strong bands at 1912 and 1587 cm^{-1}. The band at 1587 cm^{-1} is assigned to ν_{ZrH}, the stretching mode of the Zr–H bond. A number of zirconocene complexes containing terminal hydride ligands have been reported which exhibit ν_{ZrH} of energies comparable to that found for **1**.[23] Typical examples include the monomeric $Cp^*(\eta^5\text{-}C_5H_2Me_3)Zr(H)_2$ (ν_{ZrH} = 1585 cm^{-1})[23d] and dimeric $[Cp^*CpZr(H)_2]_2$ (ν_{ZrH} = 1540 (terminal) and 1270 cm^{-1} (bridging)).[23d]

Although the Zr–H stretch in **1** is found at a normal energy, the energy of the remaining band at 1912 cm^{-1} is quite low for a typical Si–H stretching frequency. Normally, ν_{SiH} for hydrosilanes are found at energies greater than 2100 cm^{-1}.[24] The energy of the absorption at 1912 cm^{-1} for **1** is significantly lower and indicates a distinct weakening of the Si–H bond. For comparison, the parent silylamine $HN^tBuSiMe_2H$ displays a Si–H stretch at 2107 cm^{-1}, almost 200 cm^{-1} greater than observed for **1**.

The infrared data for compounds **1–5** are summarized in Table 1. The Si–H stretching frequencies of all the derivatives studied are of lower energy relative to ν_{SiH} in normal hydrosilanes. The highest energy ν_{SiH} is found for fluoride derivative **5** (1998 cm^{-1}), but even this value is still 109 cm^{-1} lower than ν_{SiH} observed for $HN^tBuSiMe_2H$. The other halide derivative exhibit Si–H stretching frequencies between 1960 and 1981 cm^{-1}. We interpret the decrease in ν_{SiH} as evidence for 3c–2e$^-$ bonding in the Si–H–Zr bridge; thus the IR data yield the same trend for the strength of agostic bonding in the silylamides $Cp_2Zr(X)(N^tBuSiMe_2H)$ as determined from the NMR parameters: X = H > I > Br > Cl > F.

Molecular Structures of $Cp_2Zr(X)(N^tBuSiMe_2H)$ (X = H, Cl). Structural characterization of **1–5** in the solid state has been limited by the availability of suitable single crystals; diffraction studies were possible only for the hydride, **1**, and the chloride **4**. Although both structures suffer from configurational disordering, the disorder was modeled quite successfully in each instance, and the geometries determined appear quite reliable.

The Cp_2Zr core structure of **1** was readily located by standard crystallographic methods (see Experimental Section). The remaining atoms, however, were found to be disordered in the plane bisecting the two Cp planes (the "equatorial plane"), such that the molecule appears to possess a plane of mirror symmetry, perpendicular to the equatorial plane. This disorder is the result of the symmetrical disposition of the carbons on silicon (C15 and C16) and two of the *t*-Bu methyl carbons (C12 and C13) relative to the pseudomirror plane. As a result, these four carbon atoms appear at full occupancy, whereas the silicon atom and remaining two carbons of the *t*-Bu group appear at 50% occupancy on both sides of the mirror plane. The nitrogen atom is also disordered, although the two sites lie very close to the pseudomirror plane and are only 0.5 Å apart. The nature of this disorder is depicted in Figure 2, which shows to-scale drawings of each of the independent configurations, as well as their superposition. Note that successful refinement of all non-hydrogen atoms was achieved using this model, resulting in final agreement factors of R_1 = 0.024 and R_2 = 0.032. Not surprisingly, however, the disordered Si–H and Zr–H positions could not be reliably located from difference Fourier maps. A summary of data collection and refinement is given in Table 2, and selected bond distances and angles are listed in Tables 3 and 4. ORTEP diagrams of the configurations are shown in Figures 3 and 4.

Because C12, C13, C15, and C16 are "shared" between silicon methyl and *t*-Bu methyl sites, the observed bond distances to these atoms are somewhat anomalous. The average Si–C distance of 1.69 Å is much shorter than normal Si–C single-bond lengths (~1.82–1.90 Å).[25] Likewise, the average C–C distance involving methyl groups bound to C11 (i.e., C12 and C13, or C15 and C16) is 1.65 Å, clearly too long for a normal C–C bond. Note, however, that the bond to the unique (unshared) methyl group (C14) is 1.53 Å, quite normal for a C–C single bond.

Overall, hydride complex **1** adopts a typical bent metallocene geometry, with the N, Si, Zr, and C11 atoms lying in the equatorial plane. The average Zr–C(ring) distance of 2.52 Å falls within the range observed for a variety of zirconocene complexes.[26] The average Si–N bond length of 1.70 Å is within the range observed

(22) Wray, V. In *Annual Reports on NMR Spectroscopy*; Webb, G. A., Ed.; Academic Press: New York, 1983; Vol. 14, p 1.

(23) For examples, see: (a) Weigold, H.; Bell, A. P.; Willing, R. I. *J. Organomet. Chem.* **1974**, *73*, C23. (b) Manriquez, J. M.; McAlister, D. R.; Sanner, R. D.; Bercaw, J. E. *J. Am. Chem. Soc.* **1978**, *100*, 2716. (c) Jones, S. B.; Petersen, J. L. *Inorg. Chem.* **1981**, *20*, 2889. (d) Wolczanski, P. T.; Bercaw, J. E. *Organometallics* **1982**, *1*, 793. (e) Kot, W. K.; Edelstein, N. M.; Zalkin, A. *Inorg. Chem.* **1987**, *26*, 1339.

(24) Smith, A. L. *Spectrochim. Acta* **1960**, *16*, 87.

(25) Lukevics, E.; Pudova, O.; Sturkovich, R. *Molecular Structure of Organosilicon Compounds*; Ellis-Horwood: Chichester, England, 1989.

(26) See, for example: Cardin, D. J.; Lappert, M. F.; Raston, C. L. *Chemistry of Organo-Zirconium and -Hafnium Compounds*; Ellis-Horwood: Chichester, England, 1986.

Table 2. Summary of Structure Determinations for **1** and **4**

	1	**4**
formula	$C_{16}H_{27}NSiZr$	$C_{16}H_{26}ClNSiZr$
fw	352.71	387.15
crystal dimens, mm	0.25 × 0.33 × 0.38	0.15 × 0.20 × 0.65
crystal class	monoclinic	orthorhombic
space group	*Cc* (No. 9)	*Pbca* (No. 61)
Z	4	8
a, Å	9.997(2)	8.911(1)
b, Å	19.848(2)	14.941(3)
c, Å	10.077(2)	27.472(4)
β, deg	119.73(1)	
V, Å^3	1736(1)	3658(1)
μ, cm^{-1}	6.79	7.95
D(calc), g/cm^3	1.349	1.406
F(000)	736	1600
radiation (λ, Å)	Mo K*α* (0.710 73)	Mo K*α* (0.71073)
θ range, deg	2.0–27.5	2.0–27.5
scan mode	*ω*–2*θ*	*ω*–2*θ*
h, k, *l* collected	±12, –25, ±13	+11, –19, +35
no. of reflns measd	2164	4730
no. of unique reflns	1995	4189
no. of reflns used in refinement	1768 ($I > 3\sigma$)	2554 ($I > 3\sigma$)
no. of params	206	190
data/param ratio	8.6	13.4
R_1	0.024	0.031
R_2	0.032	0.038
GOF	1.194	1.185

Table 3. Bond Distances (Å) in **1**[a]

Zr–Si	2.857(2)	Zr–Si′	2.853(2)
Zr–N	2.143(6)	Zr–N′	2.230(7)
Si–N	1.709(6)	Si′–N′	1.682(5)
Si–C15	1.695(7)	Si′–C12	1.699(7)
Si–C16	1.692(6)	Si′–C13	1.691(5)
N–C11	1.475(8)	N′–C11′	1.444(11)
C11–C14	1.546(16)	C11′–C14′	1.512(13)
C11–C12	1.634(10)	C11′–C15	1.664(9)
C11–C13	1.667(9)	C11′–C16	1.636(11)
Zr–C1	2.534(4)	C1–C2	1.390(8)
Zr–C2	2.519(4)	C1–C5	1.410(6)
Zr–C3	2.528(4)	C2–C3	1.393(7)
Zr–C4	2.524(4)	C3–C4	1.408(7)
Zr–C5	2.534(4)	C4–C5	1.394(9)
Zr–C6	2.523(4)	C6–C7	1.408(7)
Zr–C7	2.523(4)	C6–C10	1.396(5)
Zr–C8	2.526(5)	C7–C8	1.398(6)
Zr–C9	2.520(5)	C8–C9	1.392(6)
Zr–C10	2.518(4)	C9–C10	1.386(7)

[a] Numbers in parentheses are estimated standard deviations in the least significant digits.

Table 4. Selected Bond Angles (deg) in **1**[a]

Zr–N–Si	95.1(2)	Zr–N′–Si′	92.6(3)
Zr–N–C11	139.8(5)	Zr–N′–C11′	136.8(4)
Zr–Si–N	48.3(2)	Zr–Si′–N′	51.4(2)
Si–Zr–N	36.6(1)	Si′–Zr–N′	36.1(1)
Zr–Si–C15	123.8(3)	Zr–Si′–C12	122.3(2)
Zr–Si–C16	122.4(3)	Zr–Si′–C13	124.0(3)
N–Si–C15	118.8(3)	N′–Si′–C12	119.9(3)
N–Si–C16	121.8(3)	N′–Si′–C13	117.9(3)
C15–Si–C16	109.4(4)	C12–Si′–C13	109.7(3)
Si–N–C11	125.0(6)	Si′–N′–C11′	130.5(5)
N–C11–C14	112.5(7)	N′–C11′–C14′	111.0(7)
N–C11–C12	110.7(5)	N′–C11′–C15	113.1(6)
N–C11–C13	112.7(7)	N′–C11′–C16	111.3(7)
C14–C11–C12	101.1(8)	C14′–C11′–C15	105.0(7)
C14–C11–C13	105.0(6)	C14′–C11′–C16	101.9(8)
C12–C11–C13	114.2(6)	C15–C11′–C16	113.8(5)

[a] Numbers in parentheses are estimated standard deviations in the least significant digits.

for Si–N single bonds (1.64–1.80 Å) in silazanes[25] and is comparable to distances found in $Cp_2Zr(\eta^2\text{-}SiMe_2{=}N^tBu)(PMe_3)$ (1.687(3) Å),[11] $Cp_2Zr(\eta^2\text{-}SiMe_2{=}N^tBu)(CO)$ (1.661(4) Å),[16] and $[c\text{-}Cp_2Zr(OSiMe_2N^tBu)]_2$ (1.695(2) Å).[27]

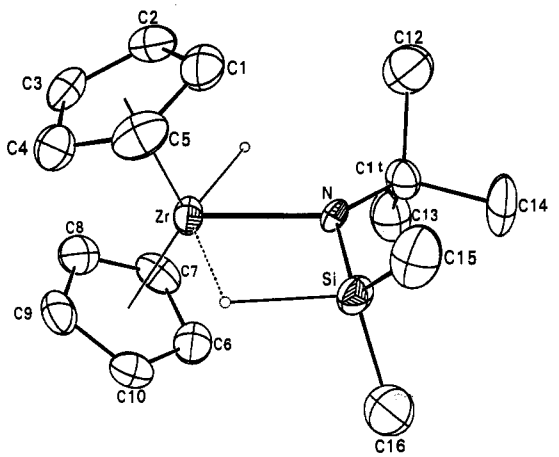

Figure 3. ORTEP drawing of $Cp_2Zr(H)(N^tBuSiMe_2H)$ (**1**), showing non-hydrogen atoms and calculated positions of the silicon and zirconium hydrides in the first disordered configuration of the silylamido fragment (see text).

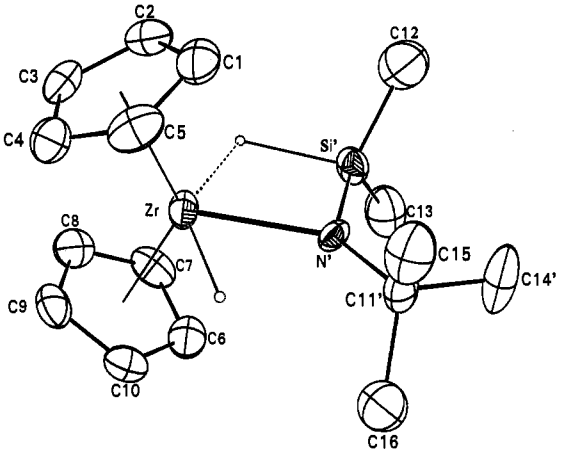

Figure 4. ORTEP drawing of $Cp_2Zr(H)(N^tBuSiMe_2H)$ (**1**), showing non-hydrogen atoms and calculated positions of the silicon and zirconium hydrides in the second disordered configuration of the silylamido fragment (see text).

As in numerous other metal amides,[28] the nitrogen atom in **1** adopts a planar geometry. The nitrogen atom lies slightly off the center of the equatorial plane, presumably due to interactions with the unlocated zirconium hydride ligand. Its position near the center of the equatorial wedge is consistent with the idea that *three* ligands lie in that plane (i.e., N, H, and η^2-SiH). If the Si–H bond were not coordinated to the Zr, the N atom would be expected to lie off the center of the equatorial plane by as much as 45°.

Perhaps the most important feature of the structure of **1**, in relation to the presence of a nonclassical interaction between the metal and the silicon hydride, is the relative positions of the Zr and Si atoms, which are separated by only 2.86 Å. Although this distance must be treated with some caution due to the disorder problem, it is remarkably short for a nonbonded contact, falling only slightly outside the range of known Zr–Si bond lengths. Only eight structurally characterized Zr–Si compounds have been reported,[11,16,29] and the Zr–Si bond lengths range from 2.654(1) Å for $Cp_2Zr(\eta^2\text{-}SiMe_2{=}N^tBu)(PMe_3)$[11] to 2.815(1) Å for Cp_2-

(27) Procopio, L. J.; Carroll, P. J.; Berry, D. H. *Organometallics* **1993**, *12*, 3087.

(28) Lappert, M. F.; Power, P. P.; Sanger, A. R.; Srivastava, R. C. *Metal and Metalloid Amides*; Ellis-Horwood: Chichester, England, 1980.

(29) (a) Muir, K. W. *J. Chem. Soc. A* **1971**, 2663. (b) Tilley, T. D. *Organometallics* **1985**, *4*, 1452. (c) Kreutzer, K. A.; Fisher, R. A.; Davis, W. M.; Spaltenstein, E.; Buchwald, S. L. *Organometallics* **1991**, *10*, 4031. (d) Heyn, R. H.; Tilley, T. D. *Inorg. Chem.* **1989**, *28*, 1768. (e) Takahashi, T.; Hasegawa, M.; Suzuki, N.; Saburi, M.; Rousset, C. J.; Fanwick, P. E.; Negishi, E. *J. Chem. Soc.* **1991**, *113*, 8564.

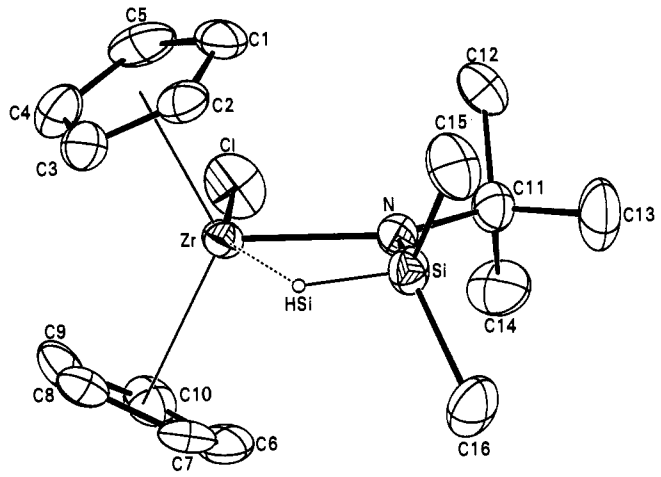

Figure 5. ORTEP drawing of $Cp_2Zr(Cl)(N^tBuSiMe_2H)$ (**4**), showing non-hydrogen atoms and the refined position of Si–H. The disordered configuration of the Cp ring (C6′–C10′) has been omitted for clarity (see text).

$Zr(SiMe_3)(S_2CNEt_2)$.[29b] In addition, the small Zr–N–Si angle (93.9°) and large Zr–N–C11 angle (138.3°) clearly show that the silicon is bent in toward the metal. In fact, the Zr–N–Si angle falls between the analogous angles for the three-membered rings of $Cp_2Zr(\eta^2\text{-}SiMe_2{=}N^tBu)(PMe_3)$ (86.1(1)°)[11] and $Cp_2Zr(\eta^2\text{-}SiMe_2{=}N^tBu)(CO)$ (89.1(2)°)[16] and the four-membered ring of $[c\text{-}Cp_2Zr(OSiMe_2N^tBu)]_2$ (96.31(8)°).[27] Although no two-center, two-electron Zr–Si bond exists in **1**, the short Zr–Si distance and acute Zr–N–Si angle strongly suggest an interaction between the two atoms, which is most easily explained by an η^2-silane bonding mode. Although neither the silicon hydride nor the zirconium hydride was located, the geometry about the silicon atom dictates that Si–H lies roughly between the Si and Zr atoms. For example, the Si–H position shown in Figure 3 was calculated on the basis of a tetrahedral silicon center and a Si–H bond length of 1.42 Å, the same distance observed in the structure of **4** (vide infra.). This places Si–H only ca. 2.1 Å from the zirconium, within the range of distances observed in bridging zirconium hydrides.[23] Three zirconocene complexes containing β-agostic hydrocarbyl ligands were structurally characterized recently. In particular, Jordan and co-workers have reported the structure of $[(MeCp)_2Zr(Et)(PMe_3)][BPh_4]$, in which a β-hydrogen of the ethyl group clearly coordinates to the cationic zirconium center.[30] The observed Zr–HC distance in this instance was 2.16 Å. In addition, Erker and co-workers have prepared and structurally characterized two agostic alkenyl complexes $Cp_2Zr(X)(R^1C{=}CR^2H)$ in which the β-CH was found in close proximity to the metal (X = Cl, 2.29 Å; Br, 2.19 Å).[31] All three of these agostic β-CH zirconocene complexes exhibit Zr–HC distances comparable to that calculated for **1**. The 1.42-Å Si–H distance assumed in the calculation above is actually rather short,[25] and a longer Si–H distance would yield an even closer Zr–H interaction.

The molecular structure of $Cp_2Zr(Cl)(N^tBuSiMe_2H)$ (**4**) was also determined by a single-crystal X-ray diffraction study. An ORTEP drawing of **4** is shown in Figure 5, and crystallographic data and important bond distances and angles are given in Tables 2, 5, and 6. Analogous to **1**, chloride complex **4** is monomeric and adopts a bent metallocene geometry in which the Cl, N, Si, Zr, and C11 atoms lie in the plane bisecting the Cp1–Zr–Cp2 angle (Cp1 and Cp2 ≡ Cp ring centroids). One of the Cp rings was found to be rotationally disordered, such that a torus of electron density is observed in the difference Fourier maps. This disorder is common to many metallocene structures and was successfully modeled with two half-occupancy Cp rings, C6–C10 and C6′–C10′. Not surprisingly, the thermal ellipsoids of these 10 sites are elongated in the direction of ring libration. The angle subtended at zirconium by the Cl and N atoms (91.1(1)°) is smaller than the value generally found in Cp_2ZrXX' derivatives (94–98°),[26] as expected if the Si–H σ-bond participates as a third ligand in the equatorial plane. The silicon hydride was located in a difference Fourier map and was successfully refined. Of course, the usual cautions regarding the accuracy of hydrogen positions in heavy-atom structures apply. In fact, the refined Si–H position yields a bond length of 1.416(31) Å, which is shorter than normal Si–H distances in hydrosilanes (1.47–1.50 Å).[25] The SiH–Zr distances is 2.266(30) Å, which is comparable to the range of distances observed in agostic Zr–HC complexes.[30,31]

The Si–N bond distance of 1.694(3) Å is normal for this type of bond[25] and is almost identical to the average value found for **1** (1.696 Å). Although a limited number of examples exist for comparison, the Zr–N distance of 2.139(3) Å falls within the range of covalent Zr–N single bonds found in other zirconocene complexes. Some examples include $Cp_2Zr(\eta^1\text{-}NC_4H_4)_2$ (2.171(2) and 2.167(2) Å),[32] $Cp_2Zr(\eta^2\text{-}PhN{=}NPh)(pyr)$ (2.161(3) and 2.105(4) Å),[33] and $Cp_2Zr(Cl)(N{=}CHMe)$ (2.013(5) Å).[34] As in hydride complex **1**, the nitrogen atom of **4** adopts a planar geometry.

The donation of electron density from the Si–H bond to the zirconium is also manifest in the Zr–Cl bond length in **4** (2.523-

Table 5. Bond Distances (Å) in **4**[a]

Zr–Cl	2.523(1)	Zr–C7′	2.502(8)	C6–C7	1.360(11)
Zr–Si	2.931(1)	Zr–C8′	2.533(8)	C6–C10	1.380(11)
Zr–N	2.139(3)	Zr–C9′	2.581(8)	C7–C8	1.405(11)
Zr–C1	2.554(4)	Zr–C10′	2.553(8)	C8–C9	1.407(11)
Zr–C2	2.545(4)	Si–N	1.694(3)	C9–C10	1.400(12)
Zr–C3	2.531(4)	Si–C15	1.854(5)	C6′–C7′	1.448(12)
Zr–C4	2.542(4)	Si–C16	1.875(4)	C6′–C10′	1.355(13)
Zr–C5	2.564(4)	Si–H	1.416(31)	C7′–C8′	1.376(12)
Zr–C6	2.538(8)	N–C11	1.494(4)	C8′–C9′	1.317(12)
Zr–C7	2.553(7)	C1–C2	1.395(5)	C9′–C10′	1.392(13)
Zr–C8	2.588(8)	C1–C5	1.391(6)	C11–C12	1.524(6)
Zr–C9	2.587(7)	C2–C3	1.371(6)	C11–C13	1.523(6)
Zr–C10	2.571(8)	C3–C4	1.376(6)	C11–C14	1.516(6)
Zr–C6′	2.549(8)	C4–C5	1.377(7)		

[a] Numbers in parentheses are estimated standard deviations in the least significant digits.

Table 6. Selected Bond Angles (deg) in **4**[a]

Cl–Zr–Si	125.9(1)	C1–C5–C4	108.1(4)
Cl–Zr–N	91.1(1)	C7–C6–C10	110.6(7)
Si–Zr–N	34.8(1)	C6–C7–C8	108.7(7)
Zr–Si–N	46.1(1)	C7–C8–C9	105.5(7)
Zr–Si–C15	123.9(2)	C8–C9–C10	109.6(7)
Zr–Si–C16	125.5(2)	C6–C10–C9	105.7(7)
Zr–Si–HSi	48.9(12)	C7′–C6′–C10′	106.6(7)
C15–Si–C16	108.4(2)	C6′–C7′–C8′	103.5(7)
N–Si–C15	119.9(2)	C7′–C8′–C9′	113.9(8)
N–Si–C16	119.0(2)	C8′–C9′–C10′	105.6(8)
N–Si–HSi	94.9(12)	C6′–C10′–C9′	110.4(8)
Zr–N–Si	99.1(1)	N–C11–C12	110.1(3)
Zr–N–C11	137.3(2)	N–C11–C13	111.3(3)
Si–N–C11	123.5(2)	N–C11–C14	109.3(3)
C2–C1–C5	107.2(4)	C12–C11–C13	106.9(3)
C1–C2–C3	107.9(3)	C12–C11–C14	110.8(3)
C2–C3–C4	108.7(4)	C13–C11–C14	108.5(3)
C3–C4–C5	108.1(4)		

[a] Numbers in parentheses are estimated standard deviations in the least significant digits.

(30) Jordan, R. F.; Bradley, P. K.; Baenziger, N. C.; LaPointe, R. E. *J. Am. Chem. Soc.* **1990**, *112*, 1289.

(31) (a) Hyla-Kryspin, I.; Gleiter, R.; Krüger, C.; Zwettler, R.; Erker, G. *Organometallics* **1990**, *9*, 517. (b) Erker, G.; Zwettler, R.; Krüger, C.; Schlund, R.; Hyla-Kryspin, I.; Gleiter, R. *J. Organomet. Chem.* **1988**, *346*, C15.

(32) Bynum, R. V.; Hunter, W. E.; Rogers, R. D.; Atwood, J. L. *Inorg. Chem.* **1980**, *19*, 2368.

(33) (a) Walsh, P. J.; Hollander, F. J.; Bergman, R. G. *J. Am. Chem. Soc.* **1990**, *112*, 894. (b) Walsh, P. J.; Hollander, F. J.; Bergman, R. G. *J. Organomet. Chem.* **1992**, *428*, 13.

(34) Erker, G.; Frömberg, W.; Atwood, J. L.; Hunter, W. E. *Angew. Chem., Int. Ed. Engl.* **1984**, *23*, 68.

(1) Å), which is significantly longer than those found in a variety of simple four-coordinate zirconocene chlorides.[26,35] Some examples include $Cp_2Zr(Cl)_2$ (2.446(5) and 2.436(5) Å),[35b] (η^5-$C_5H_4R)_2Zr(Cl)[CH(SiMe_3)_2]$ (R = ^{t}Bu, 2.452(2) Å; R = $SiMe_3$, 2.447(1) Å),[35c] and $[Cp_2Zr(Cl)]_2O$ (2.444(8) and 2.459(9) Å).[35a] Steric factors in these and a number of other complexes seem to have little influence on the Zr–Cl distance. Thus, a reasonable explanation for the observed elongation in **4** would appear to be linked to the electronic environment about zirconium. The zirconocene chlorides mentioned above are electron deficient (16-electron), coordinatively unsaturated metal complexes and are expected to behave as π-acceptors toward the chloride lone pairs. Coordination of the Si–H σ-bond to the metal in **4**, however, would lead to a more electron rich zirconium center, which should result in less π-donation from the chloride ligand and be reflected in a longer Zr–Cl linkage. Similar lengthening of the Zr–Cl bond has been observed for zirconocene chlorides which contain an intramolecularly coordinated Lewis base, such as the chelated α-alkoxyalkyl complexes $Cp_2Zr(Cl)(\eta^2\text{-}CH_2OMe)$ (2.555(1) Å),[36] $Cp_2Zr(Cl)(\eta^2\text{-}CHMeOEt)$ (2.5602(2) Å),[37] and $Cp_2Zr(Cl)(\eta^2\text{-}CH_2OCH_2Ph)$ (2.557(2) Å),[38] as well as η^2-phosphinomethanide complexes such as $Cp_2Zr(Cl)[\eta^2\text{-}C(SiMe_3)_2PMe_2]$ (2.554(1) Å).[39] A comparable lengthening of the Zr–Cl separation was also observed in the agostic alkenyl complex $Cp_2Zr(Cl)(R^1C{=}CR^2H)$ (2.550(1) Å).[31]

In addition to the long Zr–Cl distance, other indications of agostic bonding in **4** are found in the relatively short Zr–Si distance of 2.931(1) Å and the acute Zr–N–Si angle of 99.1(1)°. Combined with the large Zr–N–C11 angle of 137.2(2)°, these parameters show that the silicon atom is bent toward the metal. Although the Zr–Si distance in **4** is somewhat outside the range of known Zr–Si bond lengths (2.65–2.82 Å),[11,16,29] as well as longer than the Zr–Si interaction of **1** (2.86 Å), it is certainly short enough to be bridged by a hydrogen atom. The Zr–Si distance in **4** is slightly shorter than that in $\{Zr(Cl)(\mu\text{-}Cl)[N(SiMe_2H)_2]_2\}_2$ (2.943(1) Å), which has also been shown to have a silylamido ligand chelated to the metal via an agostic β-Si–H bond.[10] Thus, as for hydride derivative **1**, the metrical data for chloride **4** indicate that an agostic interaction between the Si–H σ-bond and zirconium is present. Consistent with the spectroscopic data discussed above, the structural parameters also suggest that this interaction is weaker in the chloride derivative than in **1**.

Conclusions: Trends and Implications of β-SiH Coordination in $Cp_2Zr(X)(N^tBuSiMe_2H)$

The spectroscopic and structural features for the series of zirconocene amides **1–5** clearly demonstrate the presence of agostic interactions between β-SiH and the metal. The nonclassical bonding mode strongly perturbs a number of spectroscopic properties, including δ_{SiH} in the ^{1}H NMR, δ_{Si} and $^1J_{SiH}$ in the ^{29}Si NMR, and ν_{SiH} in the infrared spectrum. In particular, diminished values of $^1J_{SiH}$ in **1–5**, compared to those observed for normal hydrosilanes, parallel trends found for $^1J_{HD}$ and $^1J_{CH}$ in η^2-HD and η^2-CH complexes. All of the spectroscopic parameters also show the same clear trend in the strength of the nonclassical interaction in $Cp_2Zr(X)(N^tBuSiMe_2H)$: X = H > I > Br > Cl > F.

The molecular structures of $Cp_2Zr(H)(N^tBuSiMe_2H)$ (**1**) and $Cp_2Zr(Cl)(N^tBuSiMe_2H)$ (**4**) are also consistent with coordination of the Si–H bond to the metal center. In particular, short Zr–Si distances and acute Zr–N–Si angles point to a severe bending of the silyl group toward zirconium. In addition, the location of the amido group near the center of the metallocene equatorial wedge is consistent with a Cp_2ML_3 coordination environment, not the Cp_2ML_2 geometry implied by the formula $Cp_2Zr(NR_2)(X)$. Furthermore, the silicon hydride in the structure of **4** was located in a position that is clearly bridging between the silicon and zirconium atoms.

Electron donation by the Si–H σ-bond is no doubt made possible by the electron-deficient nature of the zirconium center, and the general trends discussed above for the relative degree of agostic bonding in **1–5** mirror the electron density at the metal. Although formally 16e$^-$, electronically unsaturated complexes, the zirconium center can gain electron density through π-donation from the halide lone pairs. In the limit of complete π-donation, the zirconium would achieve an 18e$^-$ configuration and would not be expected to interact with the Si–H σ-electrons. Alternatively, in the total absence of π-donation from an ancillary ligand, the zirconium should form the strongest interaction with the Si–H bond. These extremes are depicted as the limiting resonance structures:

Consistent with this picture is that hydride derivative **1** (X = H) exhibits the strongest β-Si–H interaction, as a zirconium hydride can only act as a σ-donor toward the metal. Within the series of halide derivatives, the degree of nonclassical interaction is strongest in the iodide and weakest in the fluoride, indicating that fluoride is the best π-donor to zirconium and iodide the weakest. This is, of course, the same trend observed in boron trihalides. BF_3 is the weakest Lewis acid of that series, a fact commonly attributed to strong π-donation.[40] In this instance, π-donation overwhelms simple inductive effects, which would predict that BF_3 should be the strongest Lewis acid on the basis of electronegativities. In the case of **2–5**, the competition for the vacant orbital on zirconium between halide lone pair electrons and Si–H bonding electrons is nicely illustrated in the structure of **4**, in which the Zr–Cl distance is greatly elongated.

Recently, a great deal of interest has been focused on the dehydrogenative polymerization of hydrosilanes by electron-deficient group 4 metallocene complexes.[41] Tilley and co-workers have described model studies which suggest that four-center σ-bond metathesis pathways are operative in these reactions.[41h]

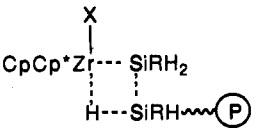

The intramolecular coordination of the β-Si–H bonds in **1–5** provides an excellent model for the viability of Zr–H–Si interactions as generally required by the Tilley mechanism. Although the Si–H complexes involve three-center interactions,

(35) For example, see: (a) Clarke, J. F.; Drew, M. G. B. *Acta Crystallogr.* **1974**, *B30*, 2267. (b) Prout, K.; Cameron, T. S.; Forder, R. A.; Critchley, S. R.; Denton, B.; Rees, G. V. *Acta Crystallogr.* **1974**, *B30*, 2290. (c) Lappert, M. F.; Riley, P. I.; Yarrow, P. I. W.; Atwood, J. L.; Hunter, W. E.; Zaworotko, M. J. *J. Chem. Soc., Dalton Trans.* **1981**, 814. (d) Bortolin, R.; Patel, V.; Munday, I.; Taylor, N. J.; Carty, A. J. *J. Chem. Soc., Chem. Commun.* **1985**, 456. (e) Bajgur, C. s.; Tikkanen, W. R.; Petersen, J. L. *Inorg. Chem.* **1985**, *24*, 2539. (f) Antiñolo, A.; Lappert, M. F.; Singh, A.; Winterborn, D. J. W.; Engelhardt, L. M.; Rasto, C. L.; White, A. H.; Carty, A. J.; Taylor, N. J. *J. Chem. Soc., Dalton Trans.* **1987**, 1463.

(36) Erker, G.; Schlund, R.; Krüger, C. *J. Chem. Soc., Chem. Commun.* **1986**, 1403.

(37) Buchwald, S. L.; Nielsen, R. B.; Dewan, J. C. *Organometallics* **1988**, *7*, 2324.

(38) Buchwald, S. L.; Nielsen, R. B.; Dewan, J. C. *Organometallics* **1989**, *8*, 1593.

(39) (a) Karsch, H. H.; Deubelly, B.; Hofmann, J.; Pieper, U.; Müller, G. *J. Am. Chem. Soc.* **1988**, *110*, 3654. (b) Karsch, H. H.; Grauvogl, G.; Deubelly, B.; Müller, G. *Organometallics* **1992**, *11*, 4238.

(40) Butler, I. S.; Harrod, J. F. *Inorganic Chemistry*; Benjamin Cummings: New York, 1989; p 110.

whereas σ-bond metathesis involves a four-centered transition state, it is certainly likely that intermolecular Si–H coordination is intimately associated with silane dehydrocoupling. It is not clear, however, whether Si–H complexes aid the catalytic process by assisting in the assembly of the four-centered transition state or actually hinder polysilane growth by providing a nonproductive thermodynamic well on the reaction coordinate. The latter case would be analogous to the situation described by Bercaw and co-workers for a scandium ethylene polymerization catalyst.[4a] In that instance, a favorable agostic β-C–H interaction with the metal in the ethyl derivative was found to significantly decrease the rate of olefin insertion and chain growth.

Experimental Section

All manipulations were carried out under an inert atmosphere in a Vacuum Atmospheres drybox or by standard Schlenk and high-vacuum line techniques. ^{1}H NMR spectra were obtained at 200, 250, and 500 MHz on Bruker AF-200, IBM AC-250, and IBM AM-500 FT NMR spectrometers, respectively. ^{13}C NMR spectra were recorded at 125 MHz on the AM-500 spectrometer, and ^{19}F NMR spectra were obtained on a Bruker WP-200 spectrometer at 189 MHz. ^{29}Si NMR spectra were obtained at 40 MHz on the AF-200 spectrometer using a DEPT pulse sequence. All NMR spectra were recorded in benzene-d_6 as solvent. Chemical shifts are reported relative to tetramethylsilane for ^{1}H, ^{13}C, and ^{29}Si NMR and external CCl_3F for ^{19}F NMR. Infrared spectra were obtained on a Perkin-Elmer Model 1430 infrared spectrometer. Solution molecular weight determinations were carried out by isothermal distillation in benzene according to the literature method.[42] Elemental analyses were performed by Robertson Laboratory, Inc. (Madison, NJ).

All solvents were distilled from sodium benzophenone ketyl prior to use. Benzene-d_6 was dried over Na/K alloy. Methyl chloride (Aldrich) was used as received. Dibromomethane, methyl iodide (Aldrich), and perfluoro-*o*-xylene were dried over molecular sieves and degassed prior to use. $HN^tBuSiMe_2H$ was prepared according to the literature procedure.[43]

$LiN^tBu(SiMe_2H)$·THF. A THF solution of $LiN^tBu(SiMe_2H)$ was prepared by a modification of the method of Seyferth and co-workers.[43] A solution of $HN^tBuSiMe_2H$ (2.31 g, 17.6 mmol) in 40 mL of THF was stirred at 0 °C under nitrogen. A 2.5 M hexane solution of ^{n}BuLi (6.5 mL, 16.3 mmol) was slowly added. The mixture was stirred at 0 °C for 1 h and then refluxed for 2 h. The THF adduct was isolated by removal of solvent under vacuum, yielding 3.29 g (96%) of white solid. ^{1}H NMR: δ 4.92 (sept, J = 3.1 Hz, SiH), 3.66 (m, α-CH_2 of THF), 1.48 (s, N^tBu), 1.28 (m, β-CH_2 of THF), 0.48 (d, J = 3.1 Hz, $SiMe_2$). Integration of peaks is consistent with the presence of one THF molecule per $LiN^tBu(SiMe_2H)$. $^{13}C\{^1H\}$ NMR: δ 68.6 (α-C of THF), 52.8 ($NCMe_3$), 37.3 ($NCCH_3$), 25.3 (β-C of THF), 5.7 ($SiMe_2$). ^{29}Si NMR: δ –28.2 (d of sept, $^1J_{SiH}$ = 164.9 Hz, $^2J_{SiH}$ = 6.3 Hz). IR (benzene): 2000 cm^{-1} (ν_{SiH}).

$Cp_2Zr(H)(N^tBuSiMe_2H)$ (1). A suspension of $[Cp_2ZrHCl]_n$ (2.30 g, 8.97 mmol) in 125 mL of benzene was stirred under nitrogen while a solution of $LiN^tBu(SiMe_2H)$·THF (1.78 g, 8.50 mmol) in 50 mL of benzene was slowly added at room temperature. After 4.5 h of stirring, the cloudy solution was filtered. Solvent was removed in vacuo, leaving an off-white solid, which was recrystallized from toluene, yielding 2.56 g of **1** (86%). Anal. Calcd for $C_{16}H_{27}NSiZr$: C, 54.49; H, 7.71. Found: C, 54.71; H, 7.95. ^{1}H NMR: δ 5.69 (s, Cp), 5.53 (d, J = 3.1 Hz, ZrH), 1.23 (s, N^tBu), 1.21 (m, SiH, obscured by N^tBu resonance), 0.04 (d, J = 2.8 Hz, $SiMe_2$). $^{13}C\{^1H\}$ NMR: δ 105.6 (Cp), 55.1 ($NCMe_3$), 34.7 ($NCCH_3$), 0.5 ($SiCH_3$). ^{29}Si NMR: δ –73.4 (d of sept, $^1J_{SiH}$ = 113.2 Hz, $^2J_{SiH}$ = 6.4 Hz). IR (benzene): 1912 (ν_{SiH}), 1587 cm^{-1} (ν_{ZrH}). Mass spectrum (isobutane CI), m/e: 351 (M^+). Solution molecular weight (benzene): 383.

$Cp_2Zr(I)(N^tBuSiMe_2H)$ (2). A toluene solution (30 mL) of **1** (0.643 g, 1.83 mmol) was stirred at room temperature under vacuum, and methyl iodide (2.02 mmol) was allowed to expand into the flask as a gas. The solution slowly turned yellow and the evolution of bubbles (methane) was observed. The mixture was stirred for 1.5 h, and then volatiles were removed in vacuo. The yellow solid was recrystallized from toluene, yielding 0.810 g of **2** (87%). Anal. Calcd for $C_{16}H_{26}INSiZr$: C, 40.15; H, 5.48. Found: C, 40.26; H, 5.47. ^{1}H NMR: δ 5.95 (s, Cp), 1.69 (br, SiH), 1.44 (s, N^tBu), 0.07 (d, J = 2.6 Hz, $SiMe_2$). $^{13}C\{^1H\}$ NMR: δ 113.1 (Cp), 58.0 ($NCMe_3$), 34.9 ($NCCH_3$), 1.0 ($SiCH_3$). ^{29}Si NMR: δ –62.0 (d of sept, $^1J_{SiH}$ = 118.7 Hz, $^2J_{SiH}$ = 5.9 Hz). IR (benzene): 1960 cm^{-1} (δ_{SiH}).

$Cp_2Zr(Br)(N^tBuSiMe_2H)$ (3). A benzene solution (20 mL) of **1** (0.258 g, 0.732 mmol) and CH_2Br_2 (0.640 g, 3.682 mmol) was stirred at room temperature for 45.5 h. Volatiles were removed in vacuo. The residue was recrystallized from toluene/petroleum ether, yielding 0.248 g of yellow **3** (79% yield). Anal. Calcd for $C_{16}H_{26}BrNSiZr$: C, 44.53; H, 6.07. Found: C, 44.21; H, 6.08. ^{1}H NMR: δ 5.94 (s, Cp), 2.24 (sept, J = 2.7 Hz, SiH), 1.43 (s, ^{t}Bu), 0.10 (d, J = 2.7 Hz, $SiMe_2$). $^{13}C\{^1H\}$ NMR: δ 113.6 (Cp), 58.0 ($NCMe_3$), 34.6 ($NCCH_3$), 1.4 ($SiMe_2$, $^1J_{SiC}$ = 57.1 Hz). ^{29}Si NMR: δ –56.1 (d of sept, $^1J_{SiH}$ = 123.2 Hz, $^2J_{SiH}$ = 6.7 Hz). IR (benzene): 1975 cm^{-1} (ν_{SiH}).

$Cp_2Zr(Cl)(N^tBuSiMe_2H)$ (4). A benzene solution (25 mL) of **1** (0.275 g, 0.780 mmol) and CH_3Cl (8.07 mmol) was stirred at room temperature for 106 h. Volatiles were removed in vacuo, and the residue was recrystallized from toluene, yielding 0.249 g of yellow **4** (83% yield). Anal. Calcd for $C_{16}H_{26}ClNSiZr$: C, 49.64; H, 6.77. Found: C, 49.70: H, 6.94. ^{1}H NMR: δ 5.93 (s, Cp), 2.58 (sept, J = 2.7 Hz, SiH), 1.41 (s, ^{t}Bu), 0.12 (d, J = 2.7 Hz, $SiMe_2$). $^{13}C\{^1H\}$ NMR: δ 113.6 (Cp), 57.8 ($NCMe_3$), 34.4 ($NCCH_3$), 1.6 ($SiMe_2$, $^1J_{SiC}$ = 56.9 Hz). ^{29}Si NMR: δ –52.3 (d of sept, $^1J_{SiH}$ = 126.5 Hz, $^2J_{SiH}$ = 6.8 Hz). IR (benzene): 1981 cm^{-1} (δ_{SiH}).

$Cp_2Zr(F)(N^tBuSiMe_2H)$ (5). A benzene solution (15 mL) of **1** (0.213 g, 0.604 mmol) and perfluoro-*o*-xylene (0.54 g, 1.889 mmol) was stirred at room temperature for 2 weeks. Volatiles were removed in vacuo, and the residue was recrystallized from toluene/petroleum ether, yielding 0.114 g of white **5** (51% yield). Anal. Calcd for $C_{16}H_{26}FNSiZr$: C, 51.84; H, 7.07. Found: C, 51.45; H, 7.10. ^{1}H NMR: δ 6.00 (s, Cp), 2.84 (d of sept, J_{HH} = 2.9 Hz, J_{FH} = 8.1 Hz, SiH), 1.33 (s, ^{t}Bu), 0.17 (d, J_{HH} = 2.9 Hz). ^{19}F NMR: δ 51.72 (d, J_{FH} = 8.1 Hz). $^{13}C\{^1H\}$ NMR: δ 112.9 (Cp), 57.2 ($NCMe_3$), 34.5 (d, J_{FC} = 4.5 Hz, $NCCH_3$), 1.3 (s, $^1J_{SiC}$ = 55.5 Hz, $SiMe_2$). ^{29}Si NMR: δ –42.0 (dd of sept, J_{SiF} = 5.1 Hz, $^1J_{SiH}$ = 135.4 Hz, $^2J_{SiH}$ ~ 6.5 Hz). IR (benzene): 1998 cm^{-1} (ν_{SiH}).

Structure Determinations of 1 and 4. General Crystallographic Procedures. Single crystals of **1** and **4** were grown from toluene/petroleum ether at –35 °C under nitrogen. Crystals of suitable size, sealed under nitrogen in 0.5-mm thin-walled Pyrex capillaries, were mounted on the diffractometer. Refined cell dimensions and their standard deviations were obtained from least-squares refinement of 25 accurately centered reflections with $2\theta > 25°$. Crystal data are summarized in Table 2.

Diffraction data were collected at 295 K on an Enraf-Nonius four-circle CAD-4 diffractometer employing Mo Kα radiation filtered through a highly oriented graphite crystal monochromator. The intensities of three standard reflections measured at intervals of ca. 80 reflections showed no systematic change during data collection. Data collection parameters are summarized in Table 2. The raw intensities were corrected for Lorentz and polarization effects by using the program BEGIN from the SDP+ package.[44] An empirical absorption correction based on ψ scans was applied.

All calculations were performed on a DEC Microvax 3100 computer with the SDP+ software package.[44] The full-matrix least-squares refinement was based on F, and the function minimized was $\sum w(|F_o| - |F_c|)^2$. The weights (w) were taken as $4F_o^2/(\sigma(F_o^2))^2$, where $|F_o|$ and $|F_c|$ are the observed and calculated structure factor amplitudes. Atomic scattering factors and complex anomalous dispersion corrections were taken from refs 45–47. Agreement factors are defined as $R_1 = \sum||F_o| - |F_c||/\sum|F_o|$ and $R_2 = [\sum w||F_o| - |F_c||^2/\sum w|F_o|^2]^{1/2}$. The goodness of fit is

(41) For example, see; (a) Aitken, C. T.; Harrod, J. F.; Samuel, E. *J. Am. Chem. Soc.* **1986**, *108*, 4059. (b) Aitken, C. T.; Harrod, J. F.; Samuel, E. *Can. J. Chem.* **1986**, *64*, 1677. (c) Aitken, C. T.; Harrod, J. F.; Gill, U. S. *Can. J. Chem.* **1987**, *65*, 1804. (d) Harrod, J. F. *Polym. Prepr.* **1987**, 403. (e) Nakano, T.; Nakamura, H.; Nagai, Y. *Chem. Lett.* **1989**, 83. (f) Hengge, E.; Weinberger, M.; Jammegg, C. *J. Organomet. Chem.* **1991**, *410*, C1. (g) Corey, J. Y.; Zhu, X-H.; Bedard, T. C.; Lange, L. D. *Organometallics* **1991**, *10*, 924. (h) Tilley, T. D. *Acc. Chem. Res.* **1993**, *26*, 22 and references therein.

(42) Clark, E. P. *Ind. Eng. Chem., Anal. Ed.* **1941**, *13*, 820.

(43) Wiseman, G. H.; Wheeler, D. R.; Seyfert, D. *Organometallics* **1986**, *5*, 146.

(44) B. A. Frenz and Associates, Inc., College Station, TX 77840, and Enraf-Nonius, Delft, Holland.

(45) *International Tables for X-Ray Crystallography*; Kynoch: Birmingham, England, 1974; Vol. IV, Table 2.2B.

(46) Stewart, R. F.; Davidson, E. R.; Simpson, W. T. *J. Chem. Phys.* **1965**, *42*, 3175.

(47) *International Tables for X-Ray Crystallography*; Kynoch: Birmingham, England, 1974; Vol. IV, Table 2.3.1.

defined as GOF = $[\sum w(|F_o| - |F_c|)^2/(N_o - N_p)]^{1/2}$, where N_o and N_p are the number of observations and parameters.

Solution and Refinement for 1. The coordinates of zirconium were obtained from a three-dimensional Patterson map. Subsequent difference Fourier maps revealed the Cp carbons but indicated that the silylamide ligand was disordered such that the complex exhibited pseudomirror symmetry. The disorder was successfully solved using the model described under Results and Discussion, in which the silicon, nitrogen, central *t*-Bu carbon, and one *t*-Bu methyl carbon occur as two equally populated sites related by approximate mirror symmetry (Figure 2). The remaining four carbons are shared between Si methyl and *t*-Bu methyl sites. All atoms for this model were located in Fourier maps except for the two N sites, which appeared as a single atom with large Gaussian amplitudes. The two sites were therefore initially calculated relative to the *tert*-butyl groups by assuming a N–C11 distance of 1.42 Å. The independent nitrogen positions were then successfully refined. All hydrogen atoms on carbons were placed at idealized locations (d(C–H) = 0.95 Å) using the program HYDRO.[44] Hydrogens in the disordered portion of the molecule were included at 50% multiplicity. The hydrogen atoms on Zr and Si were not located in the final difference Fourier map and were not included in the final structure factor calculation. Final refinement included anisotropic thermal parameters for all non-hydrogen atoms. Final agreement factors are listed in Table 2. Listings of final positional parameters and thermal parameters for **1** are included in the supplementary material.

Solution and Refinement for 4. The coordinates of the zirconium atom were obtained from a three-dimensional Patterson map. Analysis of subsequent difference Fourier maps led to location of the remaining heavy atoms. One of the Cp rings was found to be rotationally disordered. The disorder was best modeled with two half-occupancy Cp sites rotated 36° with respect to one another (C6–C10 and C6′–C10′). All hydrogen atoms were placed at idealized locations (d(C–H) = 0.95 Å) with use of the program HYDRO.[44] Calculated hydrogens on the disordered carbons were placed at 50% occupancy. The final difference Fourier map revealed a peak in a position between the Zr and Si centers and in the equatorial plane. This peak was taken to be η^2-Si–H, and its position was successfully refined using an isotropic thermal parameter. Final refinement also included anisotropic thermal parameters for all non-hydrogen atoms. Other hydrogen atoms were included as constant contributions to the structure factors and were not refined. Final agreement factors are listed in Table 2. Listings of final positional parameters and thermal parameters for **4** are included in the supplementary material.

Acknowledgment. Financial support of this work by the National Science Foundation (Grant No. CHE-9014625) is gratefully acknowledged. D.H.B. also thanks the Alfred P. Sloan Foundation for a research fellowship, and L.J.P. thanks the University of Pennsylvania School of Arts and Sciences for a Dissertation Fellowship. We also thank Professor Arnold L. Rheingold for helpful discussions.

Supplementary Material Available: Tables of positional parameters and anisotropic thermal parameters for **1** and **4** (6 pages); listings of structure factors for **1** and **4** (25 pages). This material is contained in many libraries on microfiche, immediately follows this article in the microfilm version of the journal, and can be ordered from the ACS; see any current masthead page for ordering information.